Supporting Information

Effects of Electron-Donating and Electron-Accepting Substitution on Photovoltaic Performance in Benzothiadiazole-based A-D-A'-D-A Type Small-Molecule Acceptor Solar Cells

Namsun Yoon[a,b,†], Ji-Young Jeong[a,†], Sora Oh[a], Chang Eun Song[a,b,*], Hang Ken Lee[a], Won Suk Shin[a,b], Jong-Cheol Lee[a,b], Sang-Jin Moon[a,b], and Sang Kyu Lee[a,b,*]

[a]Energy Materials Research Center, Korea Research Institute of Chemical Technology (KRICT), 141 Gajeong-ro, Yuseong-gu, Daejeon 34114, Republic of Korea

[b]Advanced Materials and Chemical Engineering, University of Science and Technology (UST), 217 Gajeong-ro, Yuseong-gu, Daejeon 34113, Republic of Korea

[†]These authors equally contributed to this work

*Corresponding authors. E-mail: songce@krict.re.kr (C. E. Song) and skyulee@krict.re.kr (S. K. Lee)

Table of Contents

1. Instruments

The synthesized compounds were characterized with ^{1}H NMR and ^{1}C NMR spectra using a Bruker DPX-400 NMR Spectrometer. The UV-vis absorption spectra were recorded using a Lambda20 (Perkin Elmer) diode array spectrophotometer with chloroform solution and a thin film on a quartz substrate. Thermogravimetric analysis (TGA) was performed under a nitrogen atmosphere at a heating rate of 10 ^{o}C/min with a Dupont 9900 analyzer.

The AFM (Multimode IIIa, Digital Instruments) was operated in tapping mode to acquire images of the surfaces of photoactive layers. Conventional transmission electron microscopy (TEM) of the optimized photoactive films was performed using a JEOL JEM-2200FS operated at 200 kV. Photovoltaic properties of OSCs were characterized under simulated 100 mW/cm^2 from a Xe arc lamp with an AM 1.5 global filter. Simulated irradiance was characterized using a calibrated spectrometer and the illumination intensity was set using an NREL-certified silicon diode with an integrated KG-5 optical filter. Before the *J-V* measurement, a shadow mask with an aperture (precise area of 9 mm^2) was used to define the effective photoactive area of each OSC. The EQE was measured by underfilling the device area using a reflective microscope objective to focus the light output from a 100W Xe arc lamp outfitted with a monocromator and optical chopper; the photocurrent was measured using a lock-in amplifier, and the absolute photon flux was determined using a calibrated silcon photodiode. All device measurements were carried out in air at room temperature.

2. Fabrication of OSCs

The OSCs were fabricated with the inverted device structure (glass/ITO/ZnO/PBDB-T:NFRA/MoO_X/Ag). **PBDB-T** polymer donor was purchased from 1-Materials and we have

synthesized **BTCPDT**, **BTCPDTO4** and **BTCPDTF** for the application in NFRA-OSCs. For BHJ (Bulk-heterojunction) solutions, the PBDB-T:NFRAs (D:A = 1:1 at concentration of 17mg/ml) photoactive materials were dissolved in chlorobenzene. The BHJ solution need to be stirred at 90 °C for 4 h. Indium tin oxide (ITO) coated glass substrates were cleaned by detergent, deionized water, acetone and IPA (isopropyl alcohol). After drying in an oven for 1 h, the ITO substrates were then subjected to a UV-ozone treatment step for 15 min to improve their work function and clearance. Next, ZnO NPs solution was spin coated on ITO substrates at 5000 rpm for 20 s and annealed at 120 °C for 15 min in atmospheric air. The PEIE solution (0.5% in ethanol) was spin-coated onto ZnO layer. Then ITO substrates coated with ZnO NPs/PEIE were transferred into a nitrogen-filled glove box. The BHJ solutions were then spin coated on top of the ZnO/PEIE layer. Finally, the samples were placed in a evaporator and 7 nm of MoO_X and 70 nm of silver were then thermally evaporated under vacuum of 2×10^{-6} Torr.

3. Measurement

Charge carrier mobility measurements:

The hole and electron mobility of active films were measured with ITO/PEDOT:PSS/photoactive films/Au and ITO/ZnO/PEIE/photoactive films/Ca/Al for the hole-only and electron-only devices, respectively, which is described by $J = 9\varepsilon_0\varepsilon_r\mu V^2/8L^3$ with SCLC model. In here, J is the current density, L is the photoactive film thickness, μ is the hole or electron mobility, ε_r is the relative dielectric constant of the transport medium, ε_0 is the permittivity of free space (8.85×10^{-12} F m^{-1}), V is the internal voltage in the device, and $V = V_{appl} - V_{bi} - V_r$, where V_{appl} is the applied voltage to the device, V_{bi} is the built-in voltage due to the relative work function difference of the two electrodes

and V_r is the voltage drop due to contact resistance and series resistance across the electrodes.

GIWAXS characterization.

2D-GIWAX measurements were performed on the PLS–II 3C beam line at the Pohang Accelerator Laboratory in Republic of Korea. The neat and blend photoactive films were coated on silicon/ZnO NPs/PEIE substrate with optimized device fabrication conditions. The monochromatic X-ray beam with intensity 11 keV was adjusted with incident angle 0.11 ^{o} ~ 0.14 ^{o} on sample with irradiation time 5-20 sec, selected to maximize the scattering intensity from the active films. The scattered X-ray patterns were recorded with charge coupled device (CCD) detector.

Cyclic Voltammetry (CV)

Cyclic voltammetry (CV) was performed using a Power Lab/AD instrument model system in 0.1M solution of tetrabutylammonium hexafluorophospate (Bu_4NPF_6) in anhydrous acetonitrile as supporting electrolyte at a scan rate of 50 mVs^{-1}. A glassy carbon disk (~ 0.05 cm^2) coated with a thin film, an $Ag/AgNO_3$ electrode, and a platinum wire were used as working electrode, reference electrode and counter electrode, respectively. The highest occupied molecular orbital (HOMO) and lowest unoccupied molecular orbital (LUMO) energy levels were calculated from the onset oxidation potential and the onset reduction potential, using the empirical relationship $E_{HOMO} = -(E_{onset,ox} - E_{1/2,ferrocene} + 4.8)$ eV and $E_{LUMO} = -(E_{onset,red} - E_{1/2,ferrocene} + 4.8)$ eV, where $E_{1/2,ferrocene}$ is obtained as 0.485 eV. $E_{onset,ox}/E_{onset,red}$ of **BTCPDT**, **BTCPDTO4** and **BTCPDTF** was obtained as 1.23 eV/-0.36 eV, 1.21 eV/-0.41 eV and 1.33 eV/-0.39 eV, respectively.

4. Materials and synthesis

The solvents and the other chemicals were obtained commercially and were used without further purification (Sigma-Aldrich and TCI).

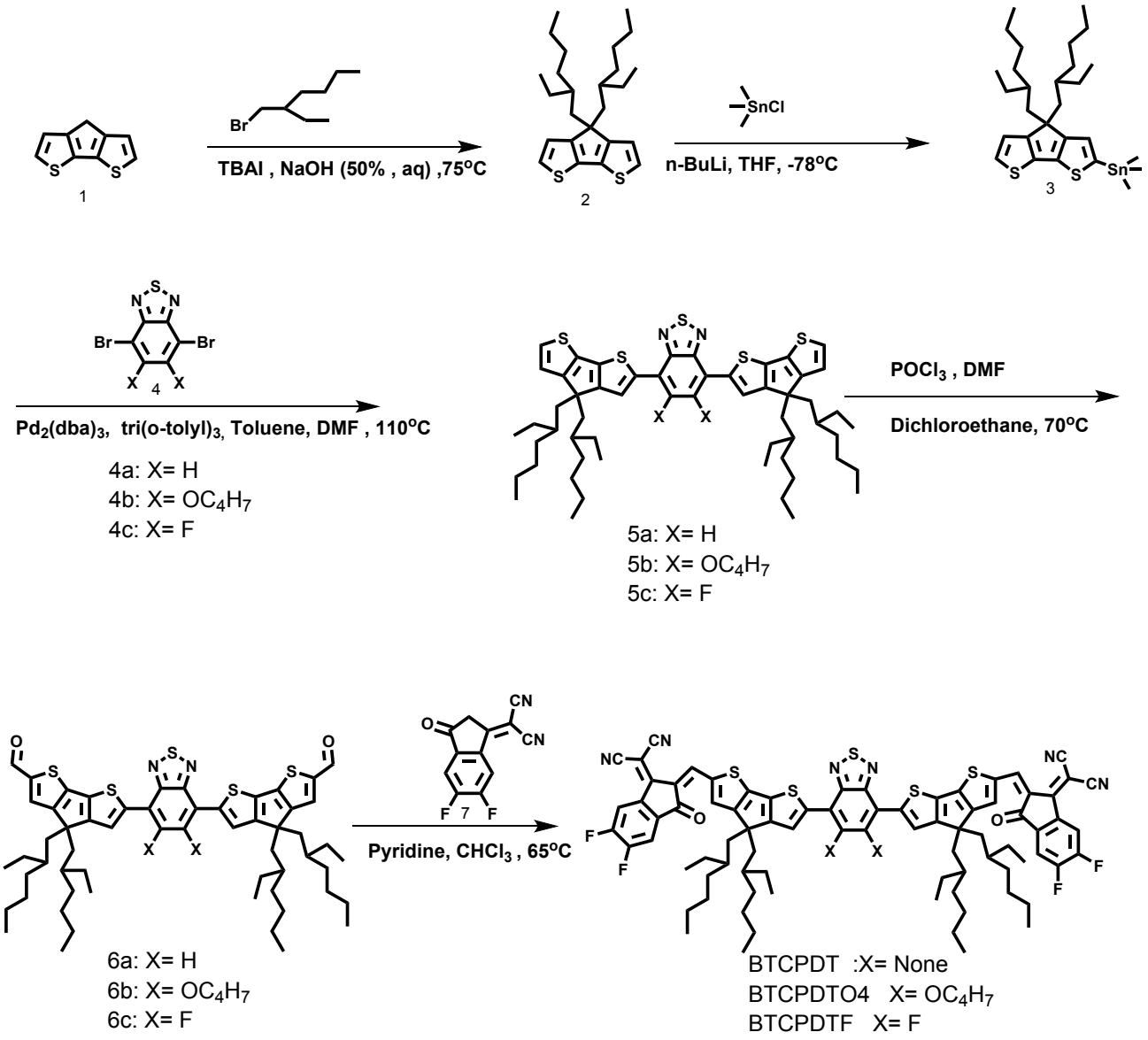

Scheme S1. Synthetic routes for A-D-A'-D-A type acceptors **BTCPDT, BTCPDTO4** and **BTCPDTF**.

Synthesis of compound 2

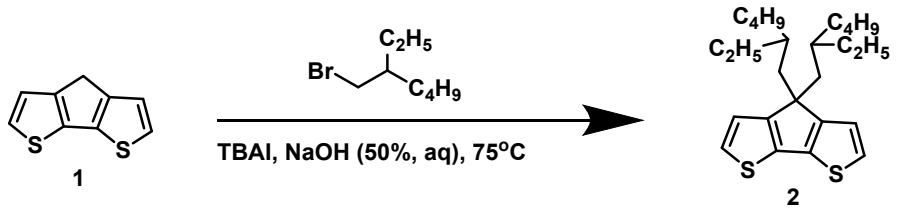

To a round bottom flask were added 1 (1 g, 5.61 mmol), tetrabutylammoniumiodide (TBAI) (361 mg, 1.12 mmol) and NaOH (20mL, 50%, aq). The mixture was deoxygenated twice with argon for 20 min followed by 3-(bromomethyl)heptane (1 g, 16.8 mmol) addition and the mixture was stirred at 75 °C for 5 h. The mixture was cooled down to room temperature and extracted with ethyl acetate (3 × 30 mL). The organic phase was dried over anhydrous $MgSO_4$ and filtered. The filtrate was concentrated under reduced pressure. The crude product was purified by column chromatography on silica gel using hexane as eluent yielding a light yellow liquid. (1.9 g, 85%) ^{1}H NMR (400 MHz, $CDCl_3$): δ = 7.10 (d, J = 4 Hz, 2H), 6.96-6.88 (m, 2H), 1.94-1.78 (m, 4H), 1.06-0.80 (m, 16H), 0.75 (m, 6H), 0.59 (m, 8H).

^{13}C NMR (101 MHz, $CDCl_3$): δ = 157.6, 136.8, 123.9, 122.3, 53.2, 43.2, 35.0, 34.1, 28.5, 28.8, 27.2, 22.7, 14.1, 10.6.

Synthesis of compound 3

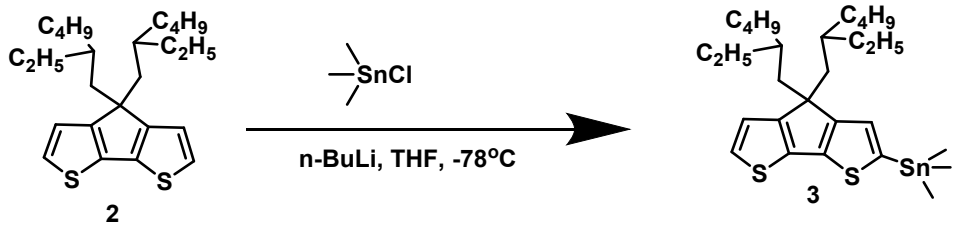

To a solution of **2** (1.9 g, 4.72 mmol) in dry THF (25 mL), n-BuLi(1.6 M; 3.1 mL) was added dropwise under nitrogen atmosphere and at a temperature of -78 °C. After stirring for 1 hours

at room temperature, trimethyltin chloride (1.0 M; 5.9 mL) was added dropwise at -78 °C. Then the mixture was stirred at room temperature for 12 hours. The mixture was poured into water and then extracted with hexane (3 × 40 mL). Then, the organic phase was dried over anhydrous $MgSO_4$ and filtered. After removing the solvent from filtrate, the product was used in the next reaction directly, yielding a brown oil (2.5 g, 93%). ^{1}H NMR (400 MHz, $CDCl_3$): δ = 7.08 (d, J = 4 Hz, 1H), 6.97-6.88 (m, 2H), 1.91-1.79 (m, 4H), 1.03-0.81 (m, 16H), 0.74 (m, 6H), 0.62-0.55 (m, 8H), 0.36 (s, 9H).

^{13}C NMR (101MHz, $CDCl_3$): δ = 159.8, 157.4, 142.4, 137.1, 136.6, 130.1, 123.9, 122.3, 52.6, 43.2, 35.1, 34.4, 34.1, 33.9, 31.6 29.7, 28.7, 28.6, 27.6, 27.3, 22.8, 22.7, 14.1, 10.7, -8.3.

Synthesis of compound 5a

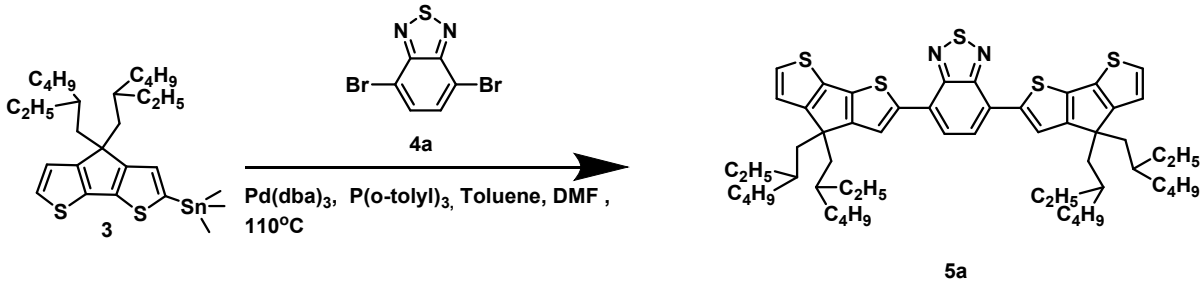

A mixture of 3 (400 mg, 0.71 mmol), 4a (75mg, 0.25 mmol) was dissolved into , toluene /DMF (4 mL/1 mL) under nitrogen protection. After $Pd(dba)_3$ (32mg, 0.03 mmol), $P(o\text{-}tolyl)_3$ (10mg , 0.03mmol)was added into the mixture, the mixture was deoxygenated with nitrogen purging for 20 minutes. The reaction mixture was stirred at 100 °C for 14 hours. After cooling down, the reaction mixture was extracted with dichloromethane (3 × 100 mL). The organic phase was dried over anhydrous $MgSO_4$ and filtered. After removing the solvent from filtrate, the crude product was purified by column chromatography on silica gel using hexane as eluent,

yielding purple solid (190 mg, 77%). ^{1}H NMR (400 MHz, $CDCl_3$): δ = 8.06(m, 2H), 7.83 (s, 2H), 7.22 (d, 2H, *J* = 4.0 Hz), 6.99 (m, 2H), 1.98 (m, 8H), 1.03–0.84 (m, 32H), 0.76 (t, *J* = 8.0 Hz, 10H), 0.64-0.55 (m, *J* = 8.0 Hz, 18H)

^{13}C NMR (101 MHz, $CDCl_3$): δ = 158.6, 158.3, 152.6, 139.1, 138.7, 137.0, 126.1, 125.3, 124.2, 122.7, 122.4, 53.7, 43.3, 35.2, 34.2, 28.7, 27.4, 22.8, 14.1, 10.7.

Synthesis of compound 5b

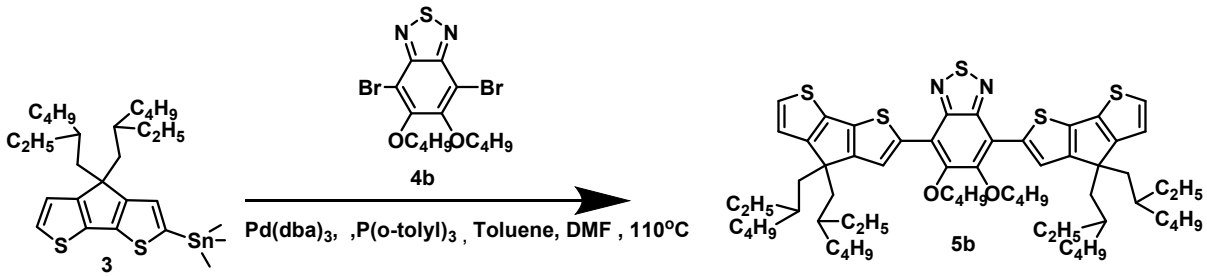

A mixture of 3 (1 g, 1.77 mmol), 4b (310 mg, 0.71 mmol), toluene/DMF (8 mL/2 mL) was dissolved into toluene /DMF (4 mL/1 mL) under nitrogen protection. After $Pd(dba)_3$ (80 mg, 0.09mmol, $P(o\text{-tolyl})_3$ (30 mg, 0.09 mmol) was added into the mixture, the mixture was deoxygenated with nitrogen purging for 20min. The reaction mixture was stirred at 100 °C for 14 hours. After cooling down, the reaction mixture was extracted with dichloromethane (3 × 100 mL). The organic phase was dried over anhydrous $MgSO_4$ and filtered. After removing the solvent from filtrate, the crude product was purified by column chromatography on silica gel using Hexane as eluent yielding purple solid (450 mg, 60%).^{1}H NMR (400 MHz, $CDCl_3$): δ = 8.60 (m, 2H), 7.20 (d, 2H, J = 4.0 Hz), 7.01 (m, 2H), 4.20 (m, 4H), 2.07-2.01 (m, 12H), 1.35-1.24 (m, 4H), 1.09-0.88 (m, 48H), 0.81-0.61 (m,18H).

^{13}C NMR (101 MHz, $CDCl_3$): δ = 159.1, 157.9. 148.9. 149.7, 141.4, 136.7, 131.1, 125.9, 125.8,

125.7, 122.4, 53.8, 43.2, 35.1, 34.2, 28.6, 27.4, 22.8, 14.1, 10.7.

Synthesis of compound 5c

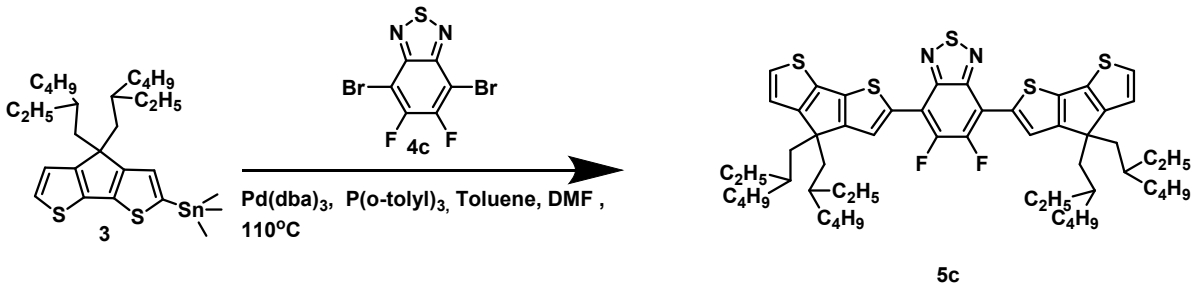

A mixture of 3 (500 mg, 0.88 mmol), 4c (102 mg, 0.31 mmol), toluene/DMF (4 mL/1 mL) was dissolved into toluene /DMF (4 mL/1 mL) under nitrogen protection. After $Pd(dba)_3$ (40mg, 0.04mmol), $P(o\text{-}tolyl)_3$ (12mg, 0.04mmol) was added into the mixture, the mixture was deoxygenated with nitrogen purging for 20 min. The reaction mixture was stirred at 100 °C for 14 hours. After cooling down, the reaction mixture was extracted with dichloromethane (3 × 100 mL). The organic phase was dried over anhydrous $MgSO_4$ and filtered. After removing the solvent from filtrate, the crude product was purified by column chromatography on silica gel using Hexane as eluent yielding purple solid (229 mg, 76%). ^{1}H NMR (400 MHz, $CDCl_3$): δ = 8.18 (t, 2H, J = 8.0 Hz), 7.23 (d, 2H, J = 4.0 Hz), 6.99 (m, 2H), 1.98 (m, 8H), 1.27 (m, 4H), 1.03–0.84 (m, 32H), 0.76 (t, J = 8.0 Hz, 12H), 0.64 (t, J = 8.0 Hz, 12H).

^{13}C NMR (101 MHz, $CDCl_3$): δ =159.1, 157.9, 149.3 (dd, $^1J_{CF}$ = 257 Hz, $^2J_{CF}$ = 20 Hz), 148.9, 141.5, 136.7, 131.2, 126.1, 125.9, 122.4, 111.7(d, $^2J_{CF}$ = 10 Hz), 53.7, 43.3, 35.2, 34.2, 28.7, 27.4, 22.8, 14.1, 10.7.

Synthesis of compound 6a

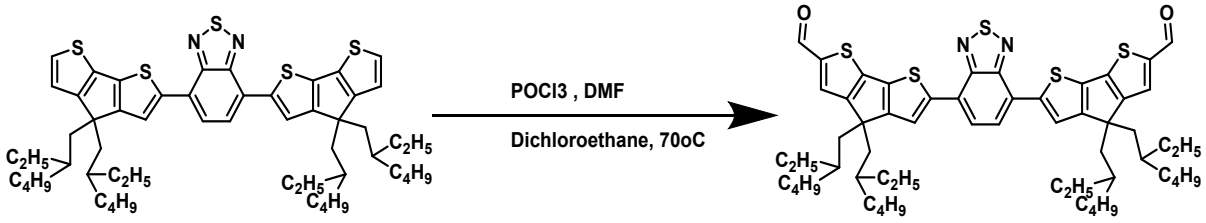

5a 6a

The 5a (190 mg, 0.20 mmol) was dissolved in dichloroethane/DMF (10 mL/2 mL) with a two-neck round-bottom flask. The mixture was cooled down to 0 °C and $POCl_3$ (0.56mL , 6 mmol)was added dropwise. After 2 hours stirring at 0 °C, the mixture was stirred at reflux for 7 hours. Saturated sodium carbonate aqueous solution (20 mL) was added and the mixture was stirred for 1hours. Then, the reaction mixture was extracted with dichloromethane (3 × 50 mL). The organic phase was dried over anhydrous $MgSO_4$ and filtered. The crude product was purified by column chromatography on silica gel using chloroform as eluent, yielding purple solid (175 mg, 88%) ^{1}H NMR (400 MHz, $CDCl_3$): δ = 9.86 (s, 2H), 8.13 (t, *J* = 8.0 Hz, 2H), 7.91 (d, *J* = 4.0 Hz, 2H), 7.61 (m, 2H), 2.03 (m, 8H), 1.03-0.89 (m, 32H), 0.75 (m, 10H), 0.68-0.57 (m, 18H).

^{13}C NMR (101 MHz, $CDCl_3$): δ = 182.2, 162.7, 158.1, 152.5, 147.6, 143.6, 137.6, 130.4, 126.3, 124.8, 122.7, 54.1, 43.3, 35.3, 34.4, 28.6, 27.3, 22.7, 14.1, 10.7.

Synthesis of compound 6b

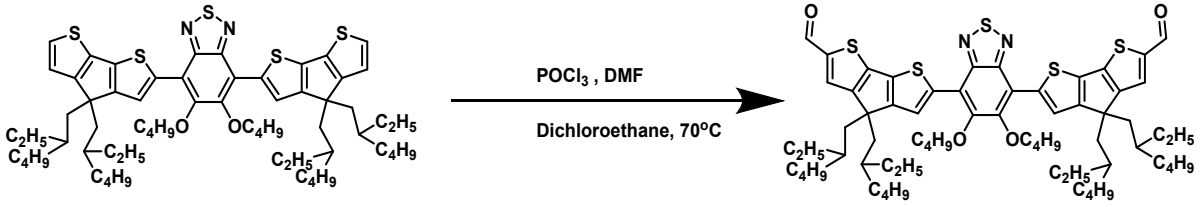

5b 6b

The 5b (220 mg, 0.20 mmol) was dissolved in dichloroethane/DMF (10 mL/2 mL) with a two-neck round-bottom flask. The mixture was cooled down to 0 °C and $POCl_3$ (0.56mL , 6 mmol) was added dropwise. After 2 hours stirring at 0 °C, the mixture was stirred at reflux for 7 hours. Saturated sodium carbonate aqueous solution (20 mL) was added and the mixture was stirred for 1 hour. Then, the reaction mixture was extracted with dichloromethane (3 × 50 mL). The organic phase was dried over anhydrous $MgSO_4$ and filtered. The crude product was purified by column chromatography on silica gel using chloroform as eluent yielding purple solid (208 mg, 91%) ^{1}H NMR (400 MHz, $CDCl_3$): δ = 9.87 (s, 2H), 8.67 (m, 2H), 7.60 (s, 2H), 4.22 (t, 4H, *J* = 8.0 Hz), 2.02 (m, 12H), 1.52 (m, 4H), 1.30–0.84 (m, 36H), 0.78-0.58 (m, 30H)

^{13}C NMR (101 MHz, $CDCl_3$): δ = 182.5, 161.7, 158.4, 151.4, 159.6, 148.1, 143.4, 138.9, 138.5, 130.6, 126.1, 117.9, 74.3, 54.1, 43.2, 35.4, 34.3, 32.4, 29.7, 28.6, 27.5, 22.7, 19.1, 14.1, 10.7.

Synthesis of compound 6c

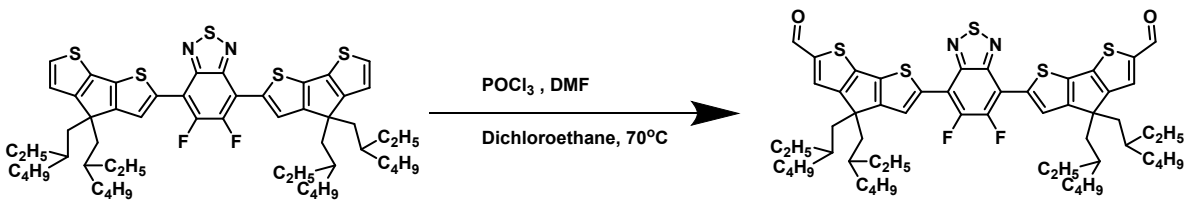

5c 6c

The 5c (229 mg, 0.23 mmol) was dissolved in dichloroethane/DMF (10 mL/2 mL) with a two-

neck round-bottom flask. The mixture was cooled down to 0 °C and $POCl_3$ (0.64mL , 6.9 mmol) was added dropwise. After 2 hours stirring at 0 °C, the mixture was stirred at reflux for 7 hours. Saturated sodium carbonate aqueous solution (20 mL) was added and the mixture was stirred for 1 hour. Then, the reaction mixture was extracted with dichloromethane (3 × 50 mL). The organic phase was dried over anhydrous $MgSO_4$ and filtered. The crude product was purified by column chromatography on silica gel using chloroform as eluent yielding purple solid (191 mg, 81%) ^{1}H NMR (400 MHz, $CDCl_3$): δ = 9.88 (s, 2H), 8.25 (t, *J* = 8.0 Hz, 2H,), 7.62 (t, 2H, *J* = 4.0 Hz), 2.03 (m, 8H), 1.27 (m, 4H), 1.12–0.86 (m, 32H), 0.76 (t, *J* = 8.0 Hz, 12H), 0.66 (t, *J* = 8.0 Hz, 12H)

^{13}C NMR (101 MHz, $CDCl_3$): δ =182.5, 161.7, 158.8, 149.9 (dd, $^1J_{CF}$ = 259 Hz, $^2J_{CF}$ = 22 Hz), 148.6, 147.1, 144.2, 140.1, 135.6, 130.5, 125.9, 112.1(d, $^2J_{CF}$ = 9 Hz), 54.1, 43.1, 35.2, 34.2, 28.7, 27.4, 22.8, 14.1, 10.7.

Synthesis of compound BTCPDT

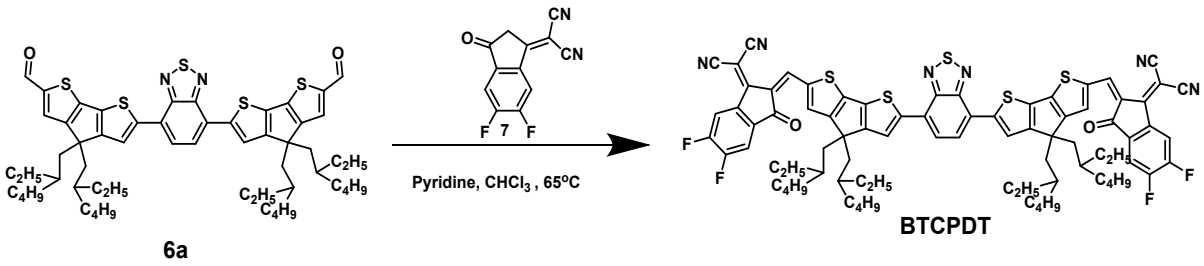

A mixture of 6a (175 mg, 0.16 mmol), 7 (162 mg, 0.70 mmol), pyridine (0.1 mL) and chloroform (10 mL) was stirred at reflux for 10hours. After cooling down to room temperature, methanol (10 mL) was added and filtered. The residue was purified by column chromatography on silica gel using chloroform as eluent yielding a deep blue solid (135 mg, 52%) ^{1}H NMR

(400 MHz, $CDCl_3$): δ= 8.91 (s, 2H), 8.55-8.48 (m, 2H), 8.27-8.20 (m, 2H), 7.97 (s, 2H), 7.76-7.64 (m, 4H), 2.09 (m, 8H), 1.12–0.84 (m, 36H), 0.77 (t, *J* = 8.0 Hz, 12H), 0.67 (t, *J* = 8.0 Hz, 12H)

^{13}C NMR (101 MHz, $CDCl_3$): δ = 186.14, 166.25, 159.99, 158.44, 155.30, 153.22 ,152.28, 147.40, 139.41, 138.56, 138.18, 136.49, 134.48, 126.61, 125.68, 123.40, 119.66, 114.98, 114.73, 112.44, 68.16, 54.21, 43.23, 35.55, 34.19, 28.49, 27.44, 22.80, 14.06, 10.65

MS (MALDI-TOF): calculated m/z: 1418.8; found [M^{+1}]: 1418.1; Anal. Calculated for $C_{82}H_{80}N_6F_4O_2S_5$ (%): C, 69.46; H, 5.68; N, 5.93; F, 5.36; O, 2.26; S, 11.31: Found (%); C, 68.72; H, 5.61; N, 5.51.

Synthesis of compound BTCPDTO4

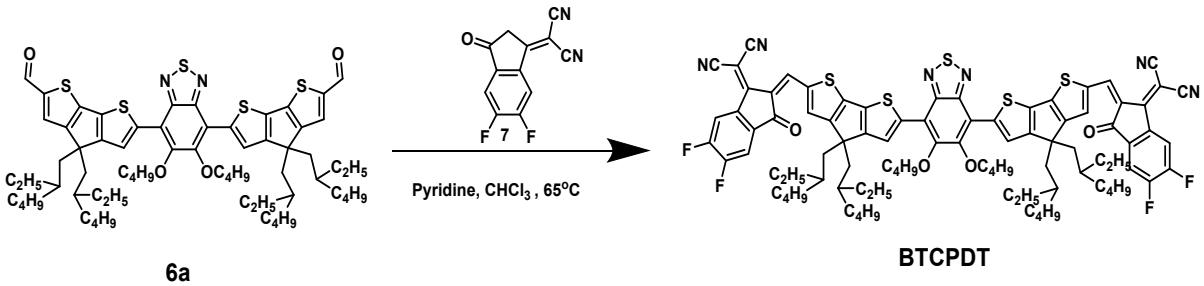

6a **BTCPDT**

A mixture of 6b (200 mg, 0.18 mmol), 7, pyridine (0.1 mL) and chloroform (10 mL) was stirred at reflux for 10 hours. After cooling down to room temperature, methanol (10 mL) was added and filtered. The residue was purified by column chromatography on silica gel using chloroform as eluent yielding a deep blue solid (154 mg, 48%) ^1H NMR (400 MHz, $CDCl_3$): δ = 8.95 (s, 2H), 8.87 (m, 2H), 8.55 (s, 2H), 7.69 (t, 4H, *J* = 8 Hz), 4.28 (t, 4H, *J* = 8.0 Hz,), 2.08 (m, 12H), 1.25–0.87 (m, 40H), 0.83-0.72 (m, 12H), 0.70-0.56 (m, 18H).

^{13}C NMR (101 MHz, $CDCl_3$): δ = 186.3, 165.5, 160.5, 155.2, 153.2, 152.1, 150.4, 143.2, 139.5,

139.3, 138.4, 138.1, 136.5, 134.5, 126.7, 119.2, 118.4, 114.9, 114.8, 112.4, 112.3, 67.8, 54.1, 43.3, 35.6, 34.3, 32.4, 31.6, 28.5, 27.5, 22.7, 19.2, 14.1, 13.9, 10.7.

MS (MALDI-TOF): calculated m/z: 1560.4; found [M^{+1}]: 1560.6; Anal. Calculated for $C_{90}H_{96}N_6F_4O_2S_5$ (%): C, 69.20; H, 6.19; N, 5.38; F, 4.86; O, 4.10; S, 10.26: Found (%); C, 69.12; H, 6.15; N, 5.14.

Synthesis of compound BTCPDTF

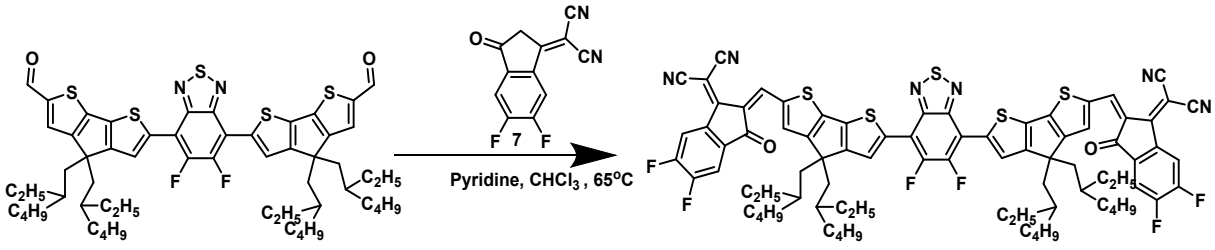

6c BTCPDTF

A mixture of 6c (190 mg, 0.18 mmol) ,7 (160 mg, 0.73 mmol), pyridine (0.1 mL) and chloroform (10 mL) was stirred at reflux for 10 hours. After cooling down to room temperature, methanol (10 mL) was added and filtered. The residue was purified by column chromatography on silica gel using chloroform as eluent yielding a deep blue solid (135 mg, 46%) ^{1}H NMR (400 MHz, $CDCl_3$): δ = 8.92 (s, 2H),8.59- 8.52 (m, 2H), 8.38-8.29 (m, 2H),7.77-7.65 (m, 4H), 2.06 (m, 8H), 1.35- 1.17 (s, 18H), 1.12–0.80 (m, 26H), 0.74 (m, 12H), 0.67 (m, 12H)

^{13}C NMR (101 MHz, $CDCl_3$): δ = 186.1, 164.8, 160.4, 158.4, 157.5, 155.3,153.2, 148.4, 140.9, 139.7, 139.2, 138.2, 136.5, 134.5, 126.2, 120.2, 114.9, 114.5, 112.5, 68.64, 54.21, 43.21, 35.54, 34.36, 34.03, 28.48, 27.55, 27.29, 22.79, 14.03, 10.63.

MS (MALDI-TOF): calculated m/z: 1453.1; found [M^{+1}]: 1453.8; Anal. Calculated for

$C_{82}H_{78}N_6F_6O_2S_5$ (%): C, 67.74; H, 5.51; N, 4.78; F, 7.84; O, 2.20; S, 11.03: Found (%); C, 62.27; H, 5.43; N, 4.67.

5. TGA, DFT calculation and CV results

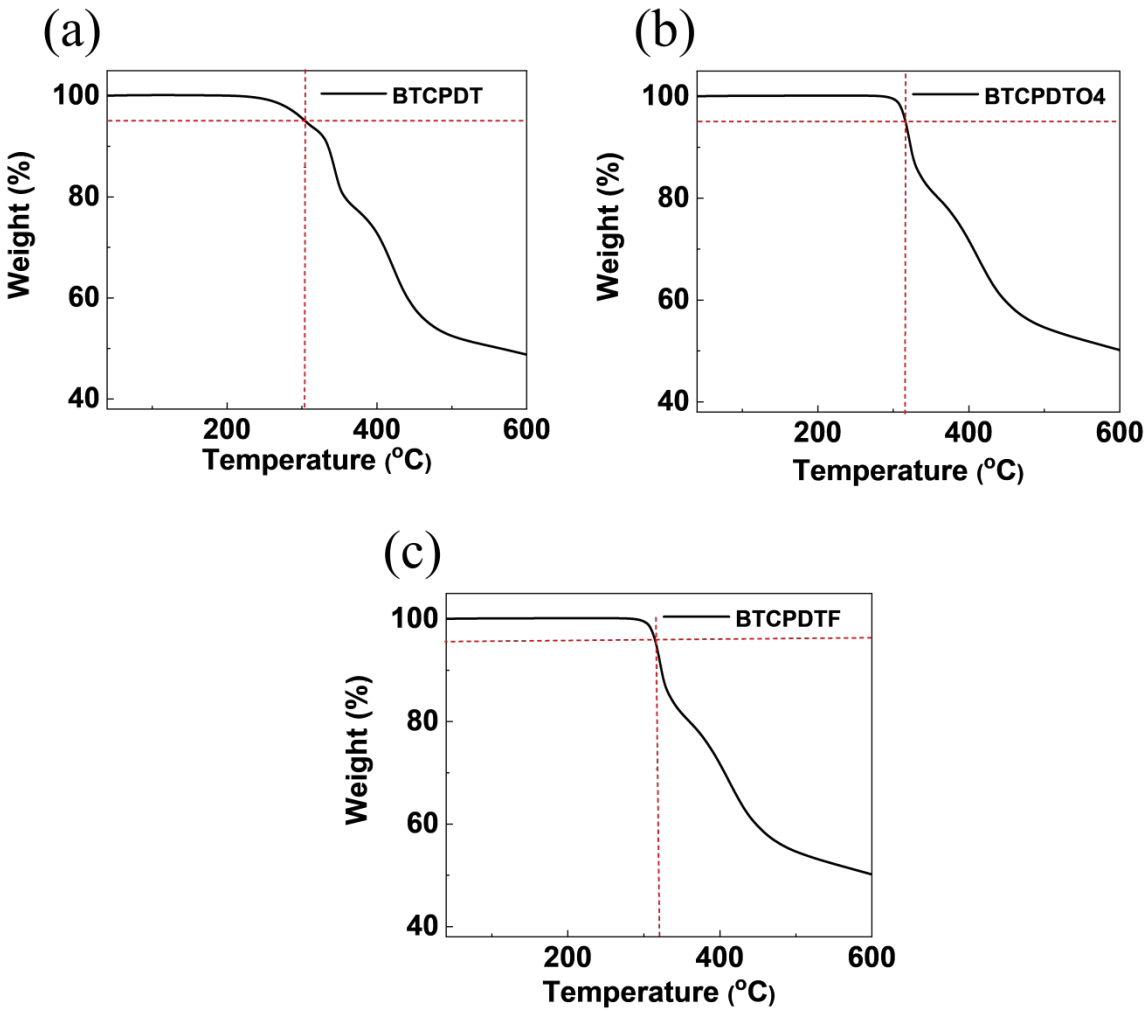

Figure S1. The TGA curves of synthesized NFRAs: (a) BTCPDT, (b) BTCPDTO4 and (c) BTCPDTF.

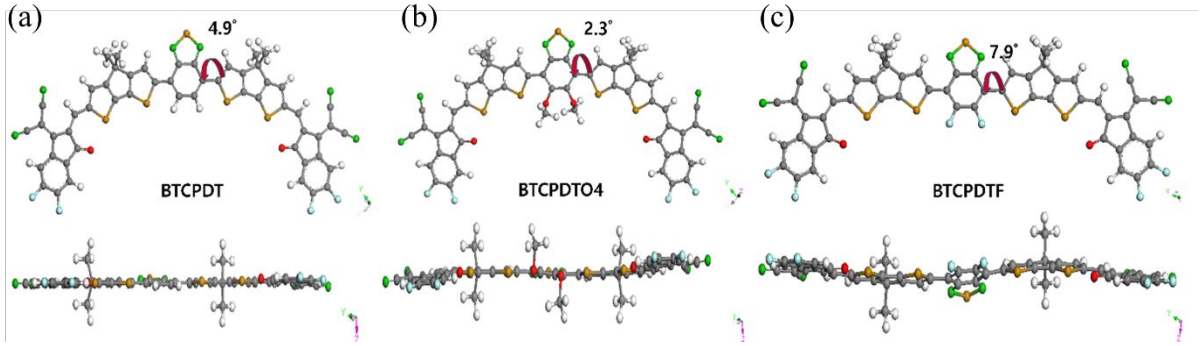

Figure S2. Top view and side view of optimized molecular geometries for (a) BTCPDT, (b) BTCPDTO4 and (c) BTCPDTF by DFT calculations with GGA function.

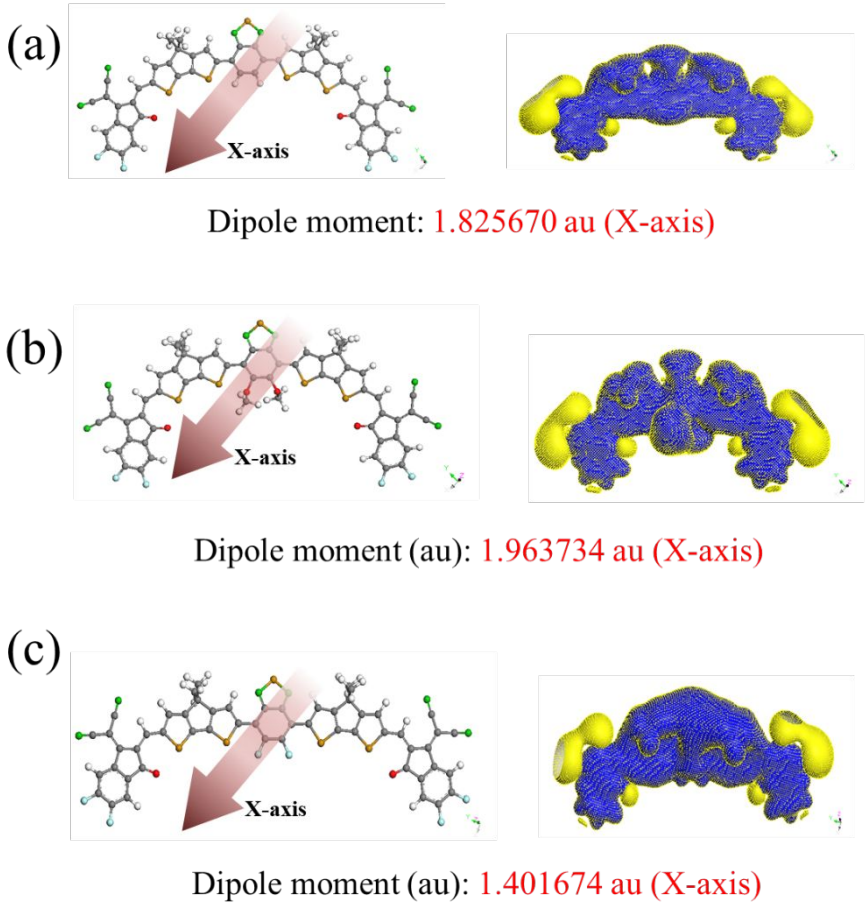

Figure S3. Schematics of the dipole moments and electronic potential surface simulated for (a) BTCPDT, (b) BTCPDTO4 and (c) BTCPDTF.

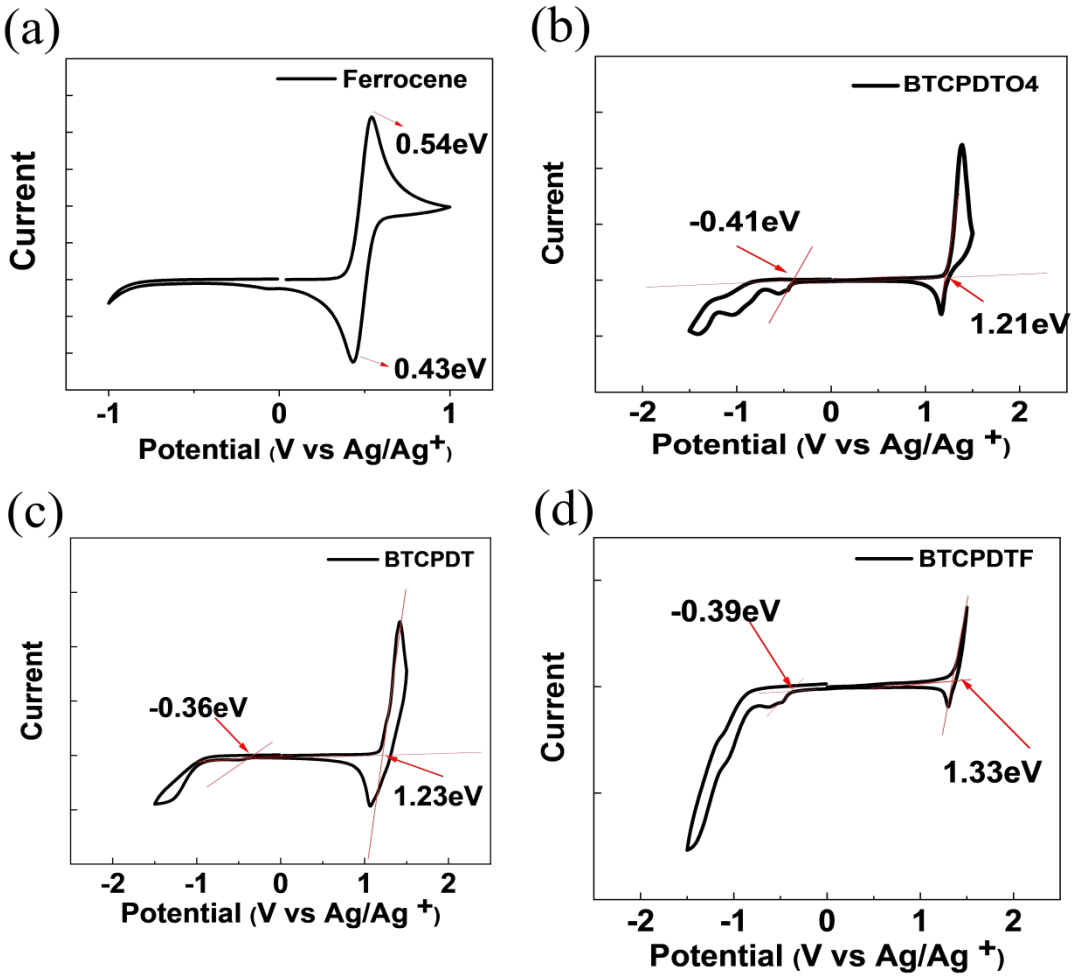

Figure S4. The CV curves for (a) Feroccene, (b) BTCPDT, (c) BTCPDTO4 and (d) BTCPDTF.

6. Optimization of efficiency in OSCs

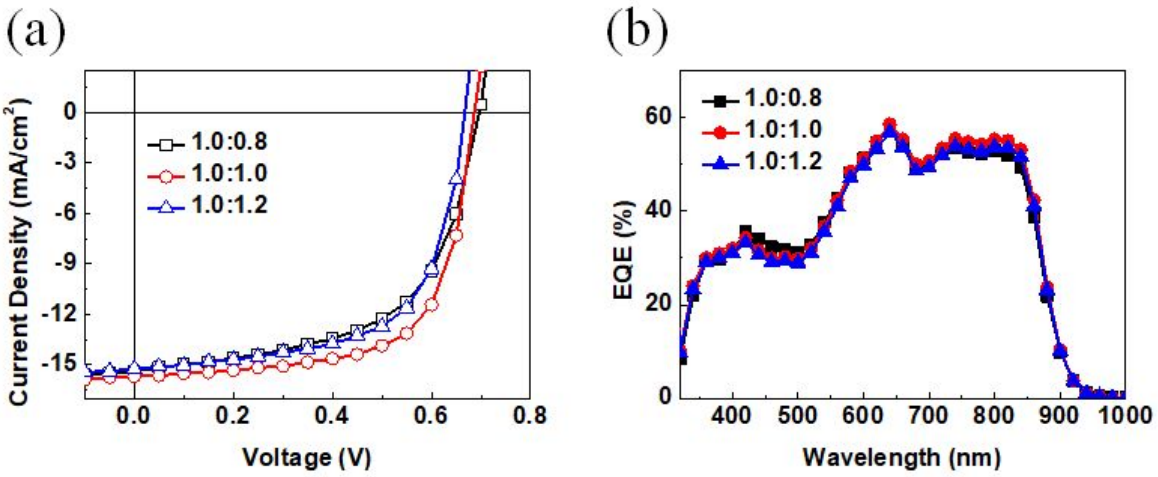

Figure S5. (a) *J-V* and (b) EQE curves of PBDB-T:BTCPDT with different weigh rat io.

Table S1. Photovoltaic peoperties of PBDB-T:BTCPDT with different weigh ratio und er AM 1.5G illumination

PBDB-T:BTCPDT	V_{OC} **[V]**	J_{SC} **[mA/cm2]**	***FF*** **[%]**	**PCE[a] [%]**
1.0:0.8	0.69	15.37 (14.80)[b]	57	6.05 (5.89±0.16)[c]
1.0:1.0	0.69	15.70 (15.07)[b]	67	7.22 (7.05±0.18)[c]
1.0:1.2	0.67	15.22 (14.65)[b]	63	6.39 (6.21±0.17)[c]

[a]Inverted device architecture is ITO/ZnO/PEIE/PBDB-T:BTCPDT (*d* = ~110nm)/MoO_X/ Ag.

[b]The value is calculated from EQE graph.

[c]The average values in the brackets are obtained from over 10 independent devices.

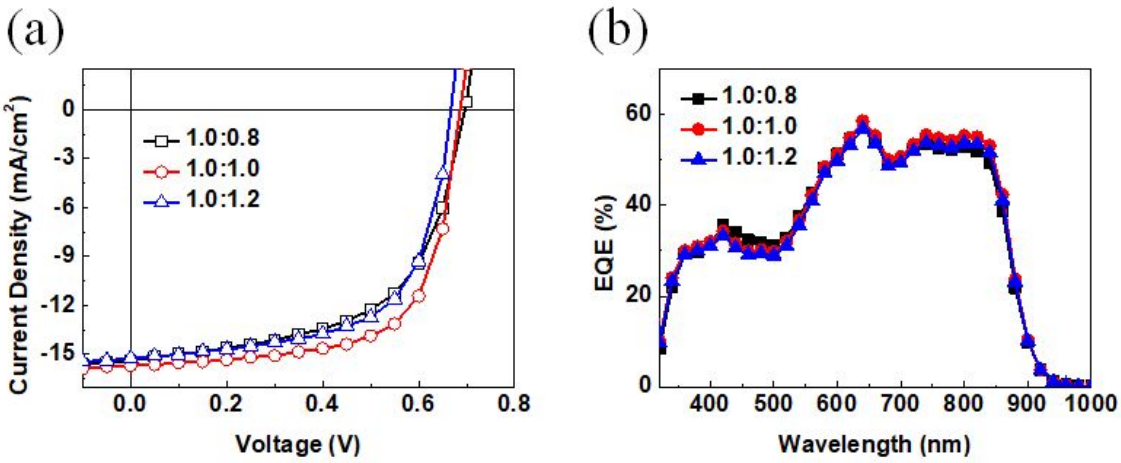

Figure S6. (a) *J-V* and (b) EQE curves of PBDB-T:BTCPDTO4 with different weigh ratio.

Table S2. Photovoltaic peoperties of PBDB-T:BTCPDTO4 with different weigh ratio under AM 1.5G illumination

PBDB-T:BTCPDTO4	V_{OC} **[V]**	J_{SC} **[mA/cm2]**	***FF*** **[%]**	**PCE[a] [%]**
1.0:0.8	0.79	20.13 (19.35)[b]	68	10.74 (10.60±0.15)[c]
1.0:1.0	0.78	21.21 (20.36)[b]	71	11.85 (11.72±0.14)[c]
1.0:1.2	0.78	20.02 (19.25)[b]	69	10.76 (10.65±0.12)[c]

[a]Inverted device architecture is ITO/ZnO/PEIE/PBDB-T:BTCPDTO4 (*d* = ~110nm)/Mo O_X/Ag.

[b]The value is calculated from EQE graph.

[c]The average values in the brackets are obtained from over 10 independent devices.

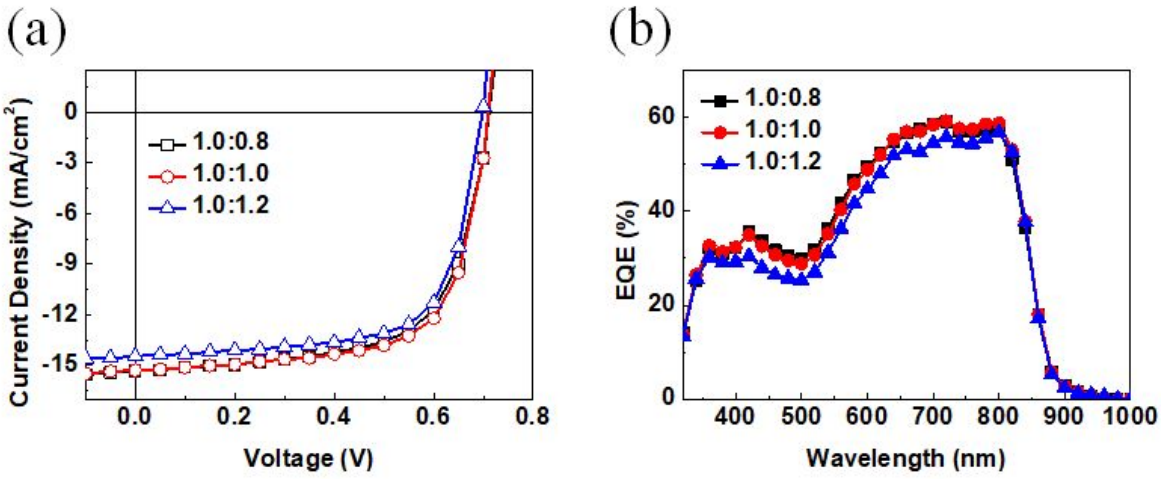

Figure S7. (a) *J-V* and (b) EQE curves of PBDB-T:BTCPDTF with different weigh r atio.

Table S3. Photovoltaic peoperties of PBDB-T:BTCPDTF with different weigh ratio un der AM 1.5G illumination

PBDB-T:BTCPDTF	V_{OC} **[V]**	J_{SC} **[mA/cm2]**	***FF*** **[%]**	**PCE[a] [%]**
1.0:0.8	0.71	15.33 (14.90)[b]	66	7.12 (6.98±0.15)[c]
1.0:1.0	0.71	15.29 (14.82)[b]	68	7.32 (7.20±0.13)[c]
1.0:1.2	0.70	14.45 (13.60)[b]	69	6.92 (6.79±0.14)[c]

[a]Inverted device architecture is ITO/ZnO/PEIE/PBDB-T:BTCPDTF (*d* = ~110nm)/MoO_X/Ag.

[b]The value is calculated from EQE graph.

[c]The average values in the brackets are obtained from over 10 independent devices.

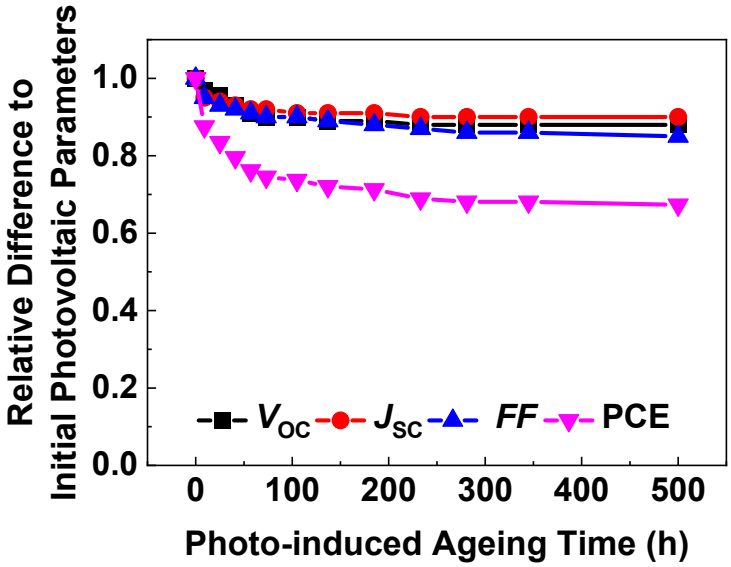

Figure S8. Normalized photovoltaic parameters as a function of photo-induced ageing time for PBDB-T:BTCPDTO4-based OSCs under continuous AM 1.5G illumination at 100 mW cm^{-2}.

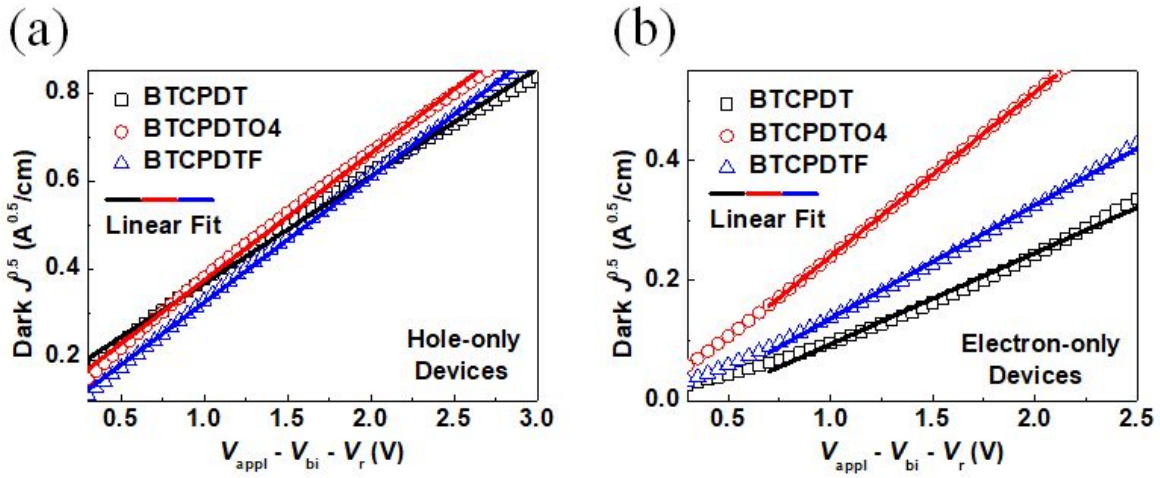

Figure S9. The dark $J^{0.5}$-V characteristics of (a) hole-only and (b) electron-only devices based on the PBDB-T:NFRAs BHJ films.

The hole and electron mobility were obtained by fitting the curves according to the Mott−Gurney equation

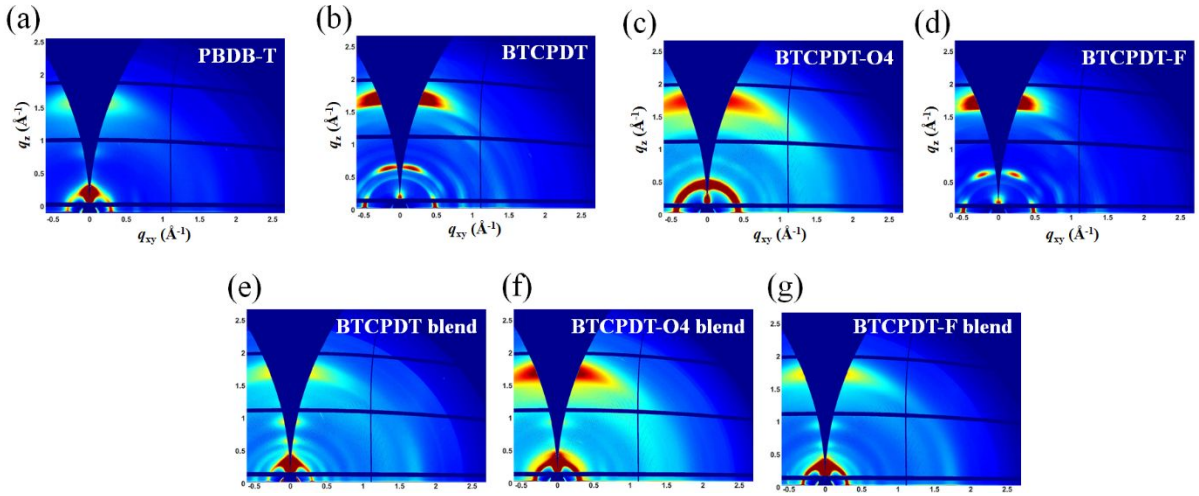

Figure S10. The 2D-GIWAXS patterns of (a-d) neat films and (e-g) PBDB-T:NFRAs blend films.

Table S4. Electron mobilities of electron-only devices with BTCPDT, BTCPDTO4 and BTCPDTF

Acceptor	**BTCPDT**	**BTCPDTO4**	**BTCPDTF**
μ_e **[cm²/V s]**[a]	6.60×10^{-4}	3.63×10^{-4}	5.47×10^{-4}

[a]The electron-only devices with structure of ITO/ZnO/PEIE/Acceptor(d = ~110 nm)/Ca/Al.

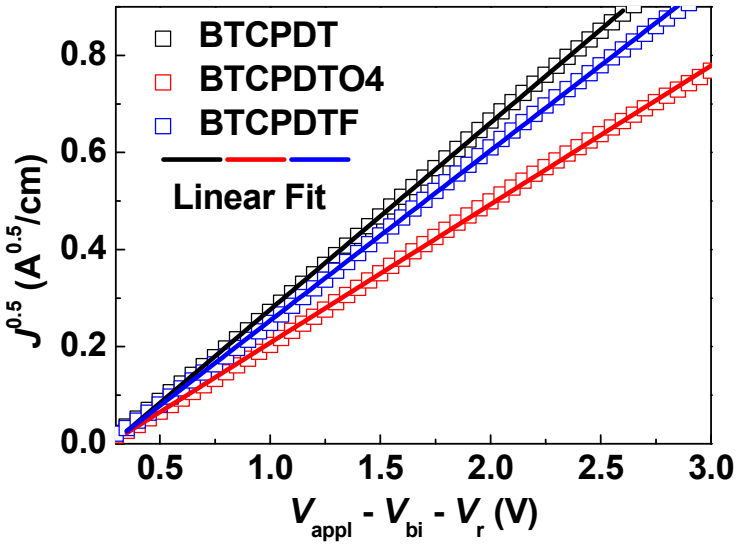

Figure S11. The dark $J^{0.5}$-V characteristics of electron-only devices based on the NFRAs neat films. The electron mobilities were obtained by fitting the curves according to the Mott−Gurney equation.

7. NMR spectra

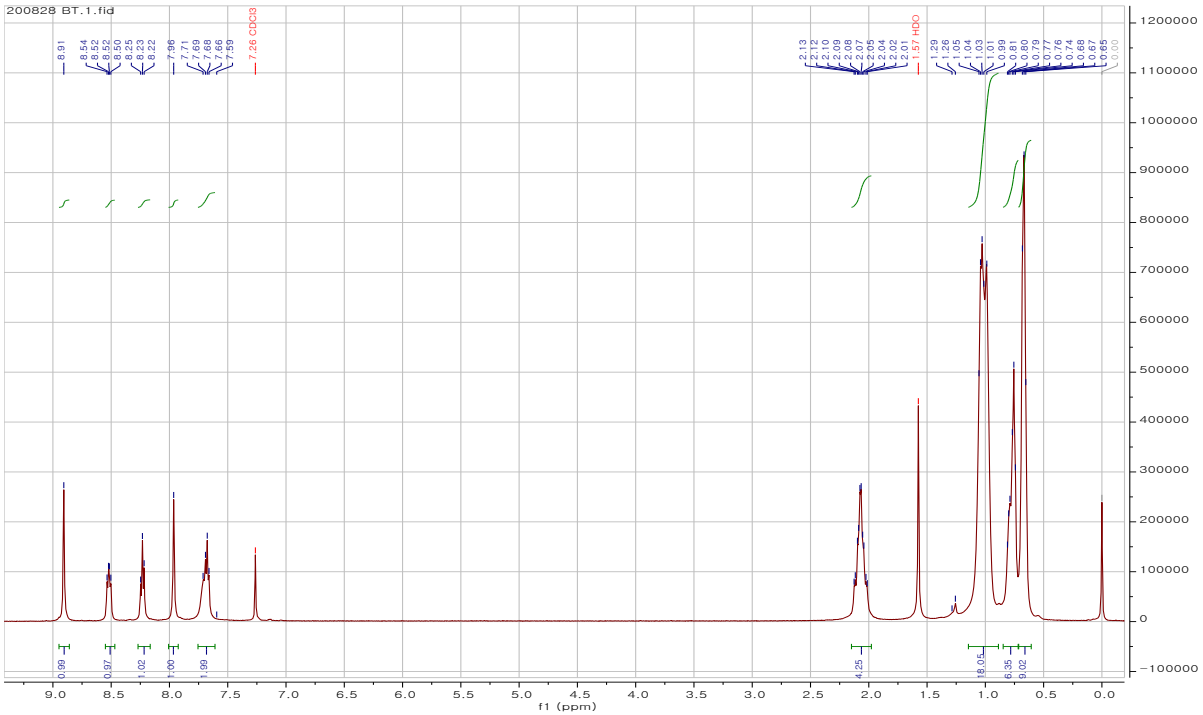

Figure S12. ^{1}H NMR spectra of **BTCPDT** in $CDCl_3$.

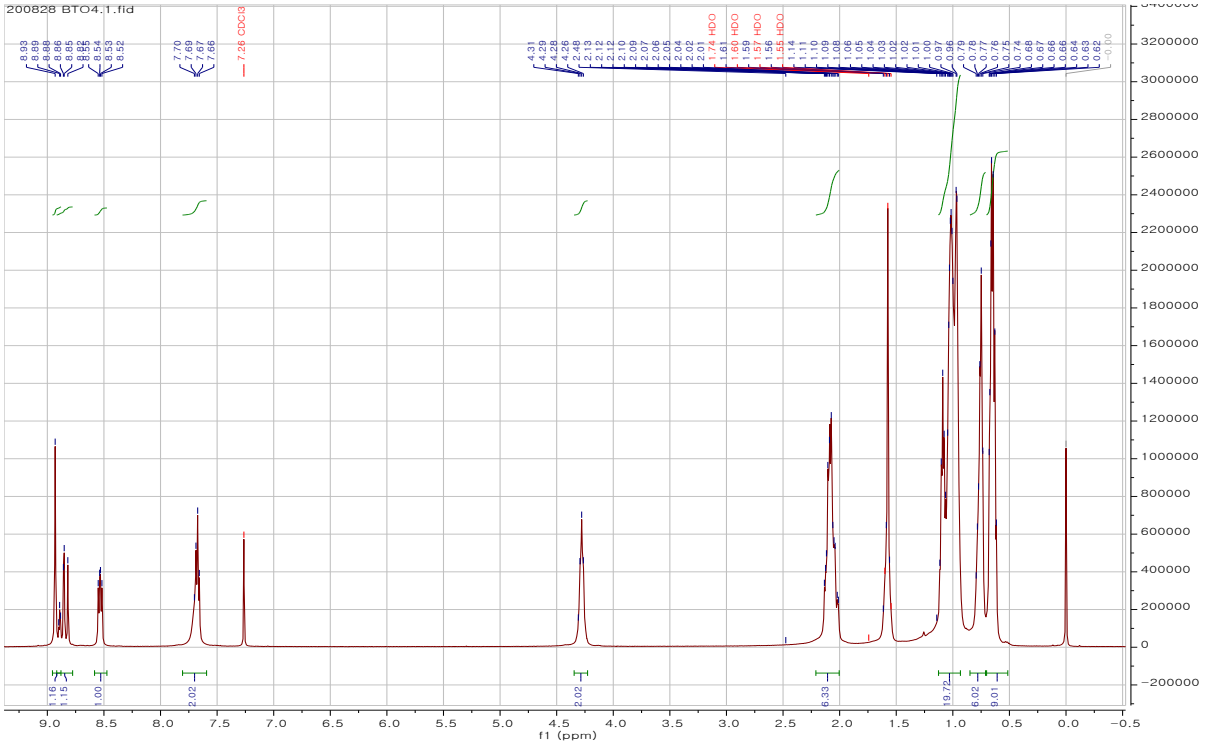

Figure S13. ^{1}H NMR spectra of **BTCPDTO4** in $CDCl_3$.

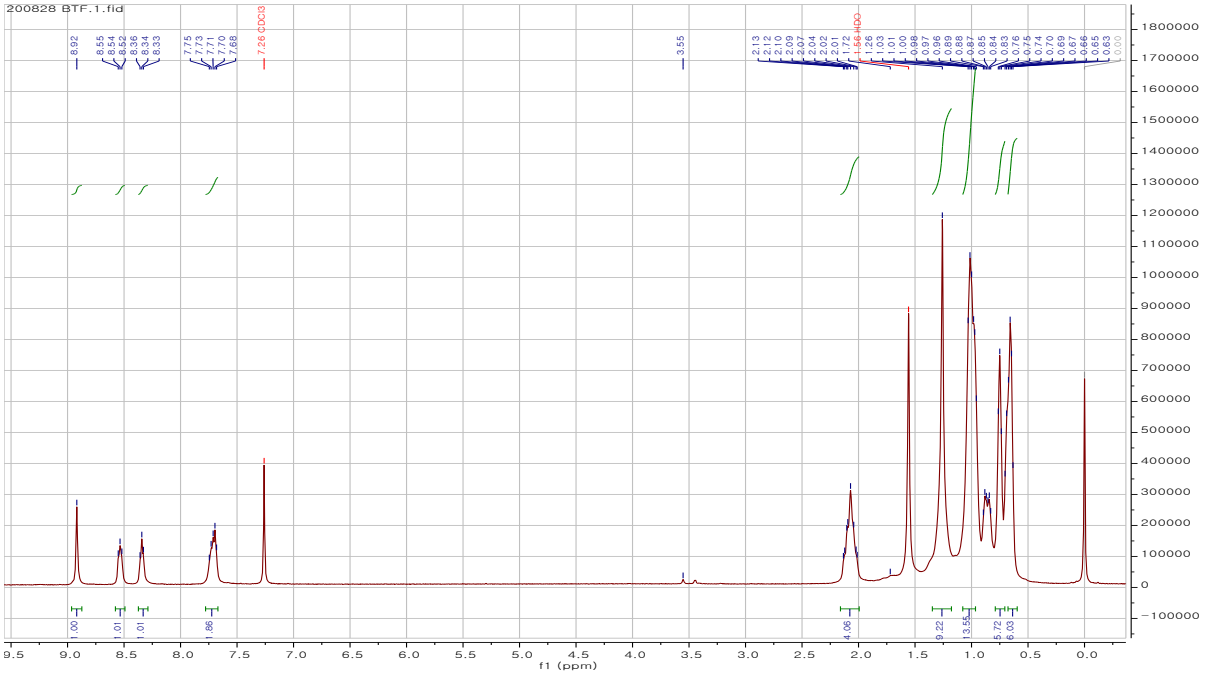

Figure S14. ^{1}H NMR spectra of **BTCPDTF** in $CDCl_3$.

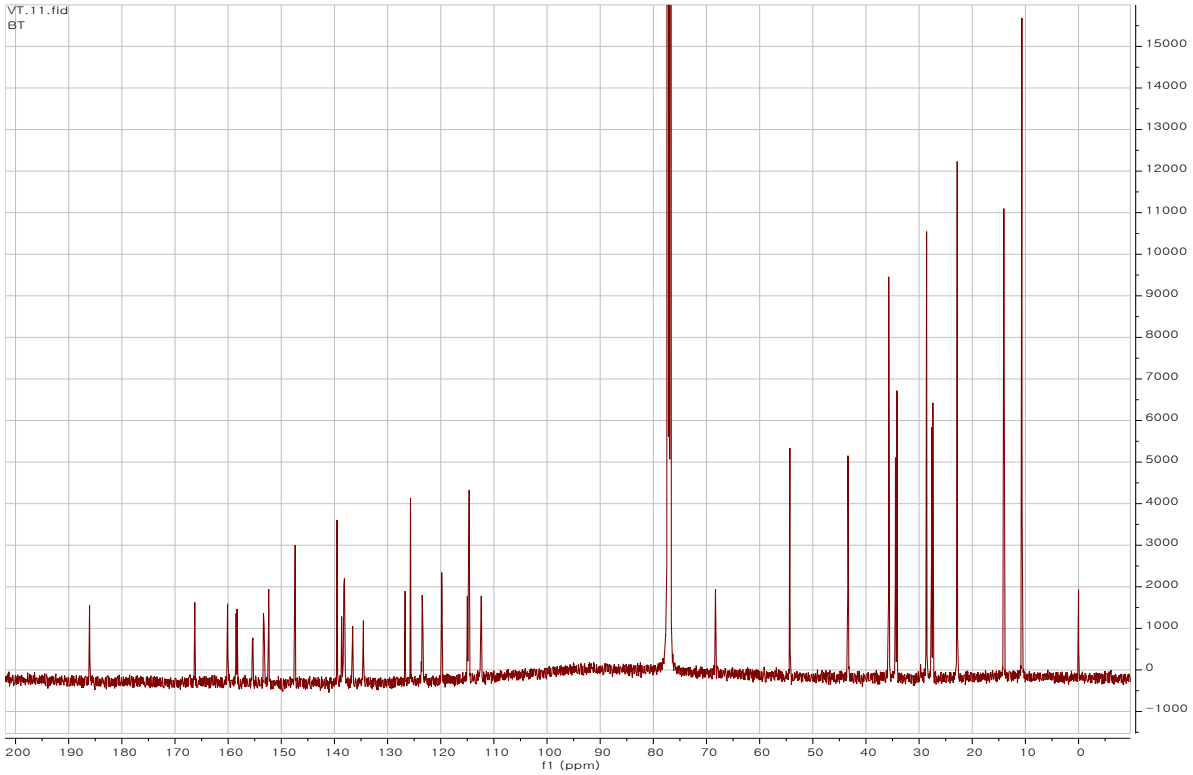

Figure S15. ^{13}C NMR spectra of **BTCPDT** in $CDCl_3$.

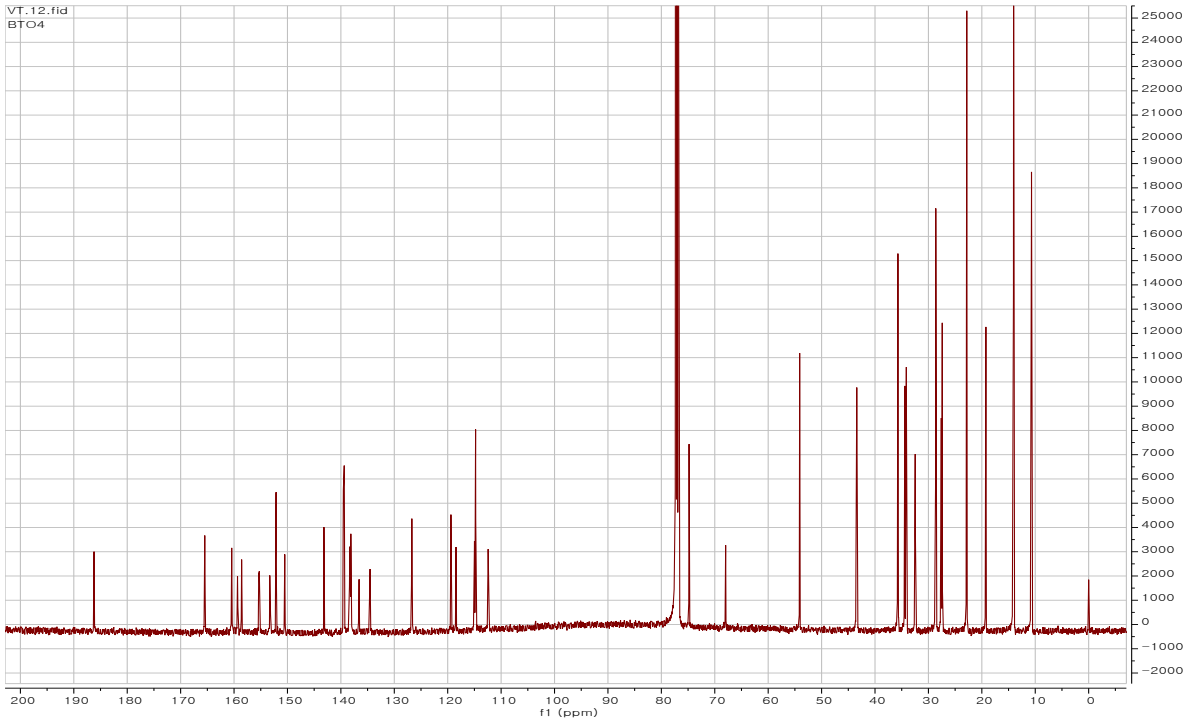

Figure S16. ^{13}C NMR spectra of **BTCPDTO4** in $CDCl_3$.

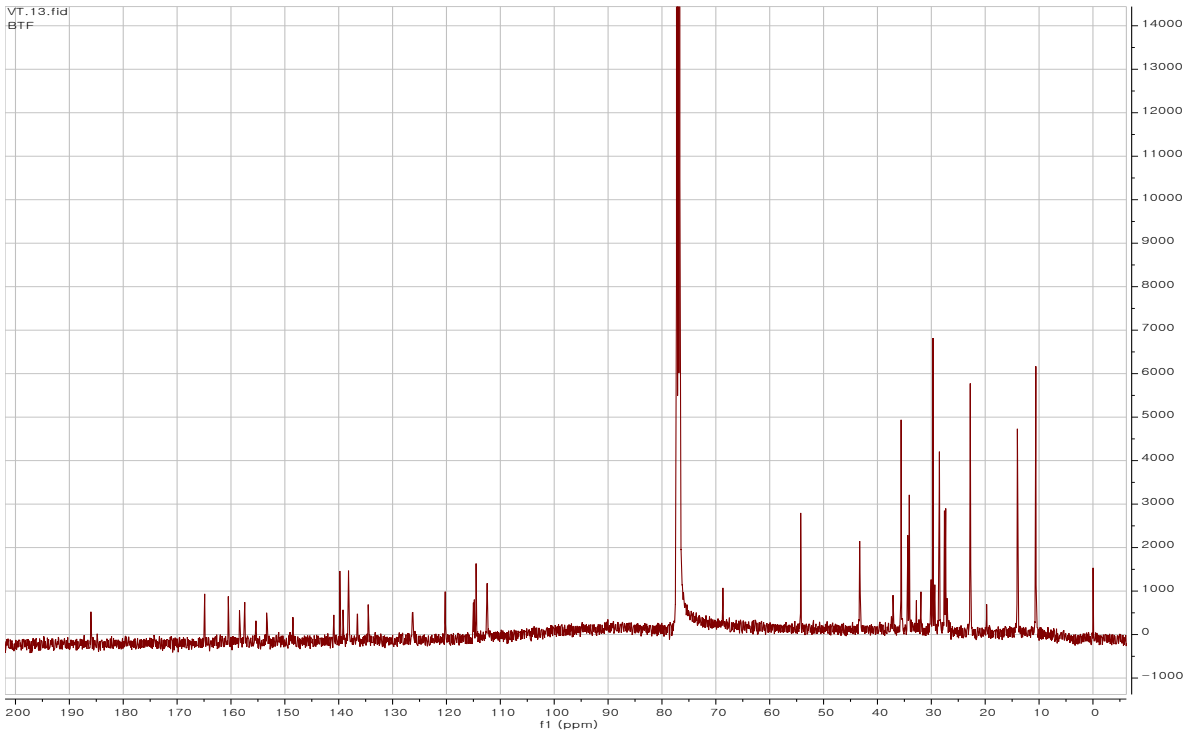

Figure S17. ^{13}C NMR spectra of **BTCPDTF** in $CDCl_3$.